IOP Conf. Series: Materials Science and Engineering **779** (2020) 012041 doi:10.1088/1757-899X/779/1/012041

Design of an optimal hydraulic tank configuration

N Belov[1,2] and N Sosnovsky[1]

[1]Bauman Moscow State Technical University

[2]E-mail: ch5n@mail.ru

Abstract. The fluid behavior in the tank of the cutting machine hydrostatic actuator is considered. The hydrodynamic simulation technique of such processes is described. The velocity magnitudes, temperature distribution fields and fluid flow lines trajectories in the tank volume analyzed. The tank configuration changes that allow to an increase its operational efficiency as the part of the hydraulic actuator are proposed. Recommendations for selecting tank optimal geometric dimensions in accordance with the criterion for the most even fluid flow rates distribution in the tank entire volume are presented.

Introduction

The tank is as a rule a thin-wall reservoir in the hydraulic system. This is a container which main tasks are storage and maintain the hydraulic actuator oil properties. Its functions efficiency depends from many factors, such as the tank cavity geometric shape, material, surface coating, specific devices presence and much more. Cases are common when the tank design is not optimal in terms of the performed functions efficiency due to the calculation methods lack or the desire to oversimplify the tank design and manufacturing progress. Such phenomenon can be much often traced in units that have been manufactured long ago but still being operated. Possible problems anticipation methods at the design stage and timely measures for its elimination are considered in this study. When upgrading the hydraulic system of a previously used but well-proven unit in order to achieve for example higher performance there are often carried out some adjustments only to the system structure and no one for the hydraulic tank so the considering question is relevant at present time. Also the similar situation occurs in case the hydraulic stations development for various reasons. It is an important to take allowance for the tank significant impact on the overall hydrostatic actuator performance.

Similar researches have been previously conducted. Various tank design tusks can be solved using CDF (Computational Fluid Dynamics) methods which are discussed in sources [1]–[9]. Flow processes numerically investigated in tanks with and without internal additional solid baffles [1]–[3]. Issues related to the dissolved gases presence in the fluid have been studied [4, 5]. The operation fluid specifications dependence from tank configuration and main flow parameters are presented in studies [3], [6]–[8].

Automated machine hydrostatic actuator components

As an example stationary hydraulic system tank optimization of the 8V66A automated cutting machine is considered [10].

Hydrostatic actuator consists of following components: vane pump type G12-22 (nominal flow rate Q = 18 l / m); hydraulic motor; executive hydraulic cylinders (for vertical and horizontal jaw vice,

circular saw lifting, work material lifting); control spool valves; pressure reducing and relief valves; throttles; fluid cooling radiators; pressure gauge and tank. The hydraulic actuator provides a quick supply, working and return headstock disk stoke, working material lifting above the bearing prism. Clamping and unclamping the work piece is carried out through a leaver system using a hydraulic cylinder.

E-20A industrial oil is used as the machine actuator's hydraulic fluid. It is a general-purpose oil without additives and has been used in hydrostatic actuators that operating indoor spaces. Main fluid specifications indicated in Table 1.

Table 1.E-20A oil main specifications.

Parameter name	Value according to GOST
Density at 20°C, kg/m^3, max	890
Density at 40°C, kg/m^3, max	859,5
Kinetic viscosity at 40°C, mm^2/s	25…35

The tank appearance one of the present hydrostatic actuator solutions is shown in Fig. 1.

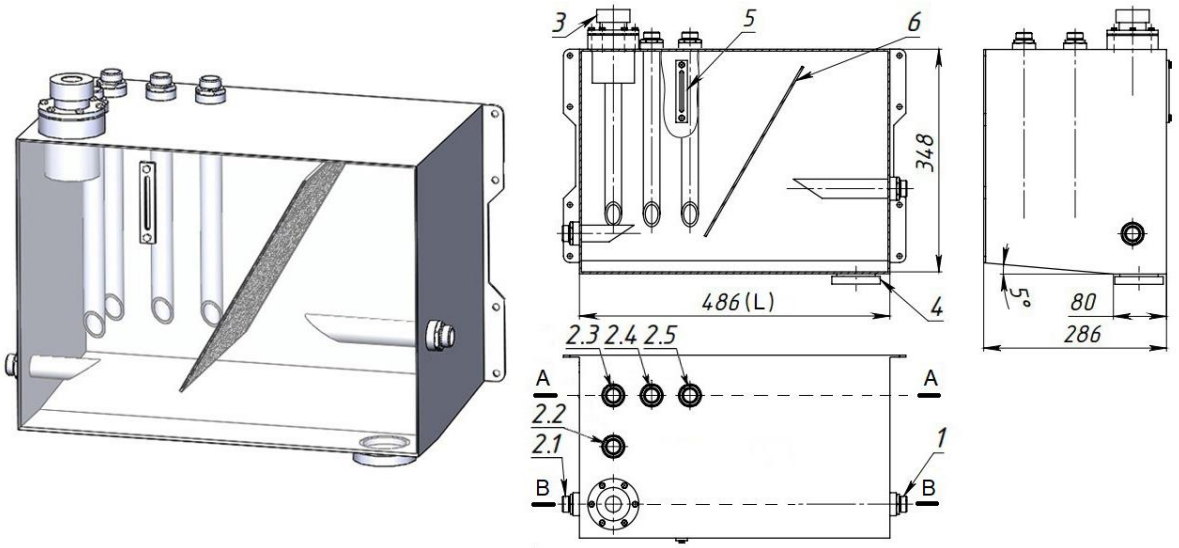

Figure 1. Tank overview and drawing

Tank parts are number-indicated: 1 — suction port; 2 — return ports (2.1 — general port of circular saw control hydraulic cylinders, 2.2 — relief valve port, 2.3 — hydraulic motor port, 2.4 — port of hydraulic cylinder horizontal vice, 2.5 — general port of vertical vice control hydraulic cylinders); 3 — tank filler opening that is combined with filler filter and breather; 4 — pollution collector bowl; fluid level indicator (32 l min, 40 l max); 6 — perforated baffle for the fluid deaeration. The tank nominal volume is 40 l (according to level indicator upper scale).

Methods

Following Favre averaged equations system describes viscous fluid hydrodynamics:

- continuity equation

$$\frac{\partial \bar{u}_i}{\partial x_i} = 0,$$

where $i = 1\ldots3$; $\bar{u}_i$ — Favre averaged stream wise$x$, y, z velocity components.

A constant density $\rho$is taken as the assumption. Thus, an incompressible Newton fluid is considered.

- momentum equation

$$\rho\left[\frac{\partial\overline{u}_i}{\partial t}+\overline{u}_j\frac{\partial\overline{u}_i}{\partial x_j}\right]=-\frac{\partial\overline{p}}{\partial x_i}+\frac{\partial}{\partial x_i}\left[T'_{ij}-\tau u_i u_j\right],$$

where $j=1\ldots3$; $\overline{p}$ — mean static pressure; $T'_{ij}=2\mu S'_{ij}$ — molecular stress tensor; μ — dynamic viscosity; $S'_{ij}=\frac{1}{2}\left[\frac{\partial\overline{u}_i}{\partial x_j}+\frac{\partial\overline{u}_j}{\partial x_i}\right]$ — strain rate pulsation tensor, $\tau u_i u_j$ — Reynolds-stress tensor.

- turbulent kinetic energy equation

$$\rho\frac{\partial k}{\partial t}+\rho\overline{u}_j\frac{\partial k}{\partial x_j}=\rho\tau_{ij}\frac{\partial\overline{u}_i}{\partial x_j}+\frac{\partial}{\partial x_i}\left[\left(\mu+\frac{\mu_T}{\sigma_{K1}}\right)\frac{\partial k}{\partial x_j}\right]-\beta_0^*\rho k\omega,$$

where $k=\frac{\left(u'_x\right)^2+\left(u'_y\right)^2+\left(u'_z\right)^2}{2}$ — turbulent kinetic energy, u'_i — stream wise x, y, z pulsation velocity components; $\mu_T=\rho\frac{k}{\omega}$ — turbulent viscosity coefficient; ω — specific dissipation rate.

- specific dissipation rate equation

$$\rho\frac{\partial\omega}{\partial t}+\rho\overline{u}_j\frac{\partial\omega}{\partial x_j}=\alpha\frac{\omega}{k}\rho\tau_{ij}\frac{\partial\overline{u}_i}{\partial x_j}+\frac{\partial}{\partial x_i}\left[\left(\mu+\frac{\mu_T}{\sigma_{\omega1}}\right)\frac{\partial\omega}{\partial x_j}\right]-\beta_0\rho\omega^2$$

Model numerical constants values are: $\beta_0^*=0,09$, $\alpha=5/9$, $\beta_0=0,075$, $\sigma_{K1}=\sigma_{\omega1}=2$.

These equations represent the k - ω turbulence model.

The laminar flow calculation can also be implemented using described mathematical model. In this case the turbulent terms of the equations tend to zero and the result is correct. The similar mathematical model was previously used for simulation flow process in positive displacement pumps [11, 12] and hydrodynamic centrifugal pumps [13]–[17] and actual results were provided.

The hydrodynamic simulation is used because this approach allows study fluid behavior in the tank cavity during the actuator operation. The occurring fluid phenomena can be sufficiently predicted. The details of the hydrodynamic simulation researches were previously considered in studies [1, 2], [5]–[9]. The described above mathematical turbulence k - ω SST model is integrated in the STAR CCM + software package.

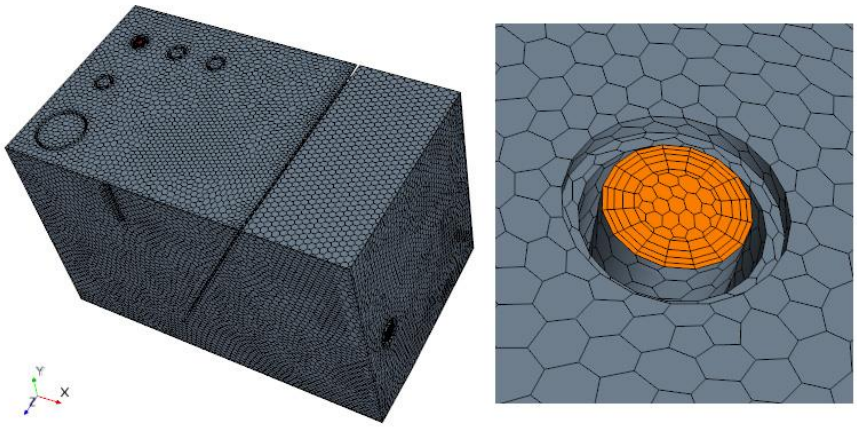

Figure 2. Fluidvolume 3dmodel

The 3dmodel of contained in the tank fluid is presented in Fig. 2.The model is divided into cells by a volumetric mesh. The cell size is selected in compliance with an acceptable relationship between the speed of the calculation process and the resulting accuracy. Nominal cell size is 6 mm. The boundary prismatic layer parameters are: cell size 50% of the nominal; the coefficient of prismatic layer extension is 1.3; prismatic layer count is 4. As an example, the prismatic layer in the suction pipe wall region is also shown in Fig. 2.

The simulation is assumed at nominal operating mode of the vane hydraulic-motor. In this case, the fluid enters the tank cavity through port 2.3 (Fig. 1). The fluid circulates in a closed circuit. Therefore the return and suction lines volume flow rates are equal. Entering fluid average temperature is T ≈ 45°C. Hydrostatic actuator pump is driven by an electric motor with a constant speed.

Boundary conditions: the velocity distribution at the pipes ports is described by a function in polar coordinate system

$$u = \begin{cases} U\left(1-\left(2r/d\right)^2\right), 0 \le r \le d \\ 0, r > d \end{cases}$$

where U — max velocity; r — radial coordinate axis; d — pipe diameter. Boundary conditions are presented in Table 2.

Table 2. Boundary conditions

U_{re}, m/s	U_{su}, m/s	d_{re}, m	d_{su}, m
1,59	1,44	$20 \cdot 10^{-3}$	$24 \cdot 10^{-3}$

The simulation is performed using following quantities:entering fluid average temperature; fluid (mineral oil) and medium carbon steel specific heat capacity, thermal conductance; fluid density and dynamic viscosity. Values are summarized in Table 3.

Table 3. Constant quantities

T_{in},°C	C_{fl},J/(kg·K)	C_{st},J/(kg·K)	K_{fl},W/(m·K)	K_{st},W/(m·K)	ρ,kg/ m^3	μ,Pa·s
45	1780	474	$9 \cdot 10^{-2}$	46	859,5	$25 \cdot 10^{-3}$

The most informative in fluid movement assessment terms are the scalar fields of the velocity distribution over sections A-A and B-B (Fig. 1), as well as flow lines in the fluid volume and the scalar heat propagation field. The simulation results are presented in Fig. 3and Fig. 4.

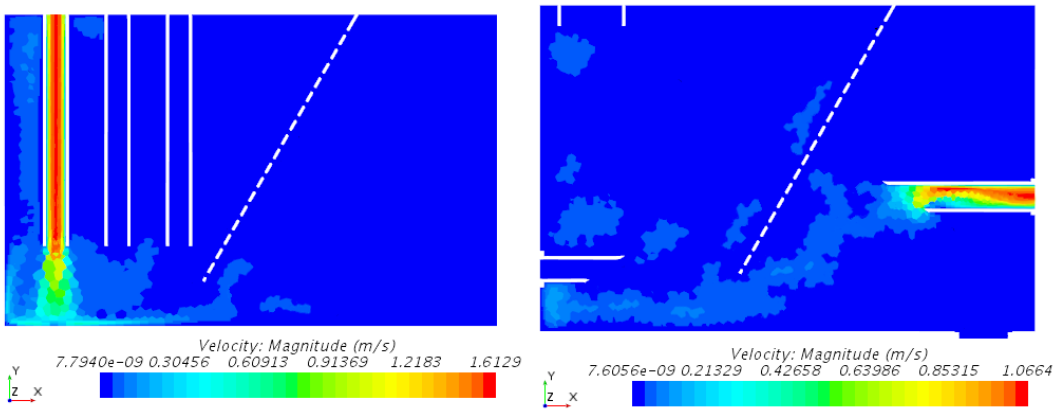

Figure3.Scalar fields of the velocity distribution over sections A-A (left) and B-B (right)

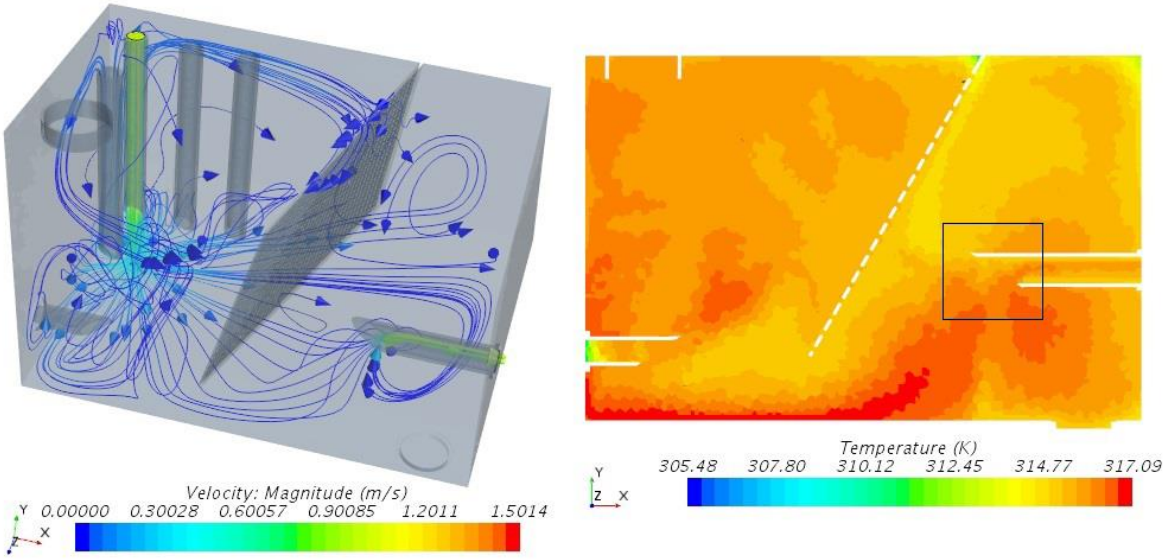

Figure 4. Flow lines (left) and scalar field of the temperature distribution over section B-B (right)

As can be seen from Fig. 3, the scalar fluid velocities distribution fields are heterogeneous: there are clearly defined regions with a more intense flow velocity and viceversa with practically zero velocity value. After entering the tank fluid immediate lyrushes to the suction pipe and only a small parts preads in the all over tank volume. Located mainly away from the suction and return line pipes fluid is less flow involved. It is necessary to study the flow lines distribution (Fig. 4) in order to unambiguous lye valuate the flow nature.

Entering the pump suction port fluid heat can be estimated as the average temperature calculated in cubic region volume near the suction pipe inlet (highlighted in a black square in Fig. 4) [18, 19].The a veragetemperatureis 315,3 K.

As the way to improve tank efficiency a nenhanced model with addition baffles which separating suction region is proposed. A tank 3dmodelis presented in Fig. 5 (1 — suction port region; 2 — inclined screen grain).

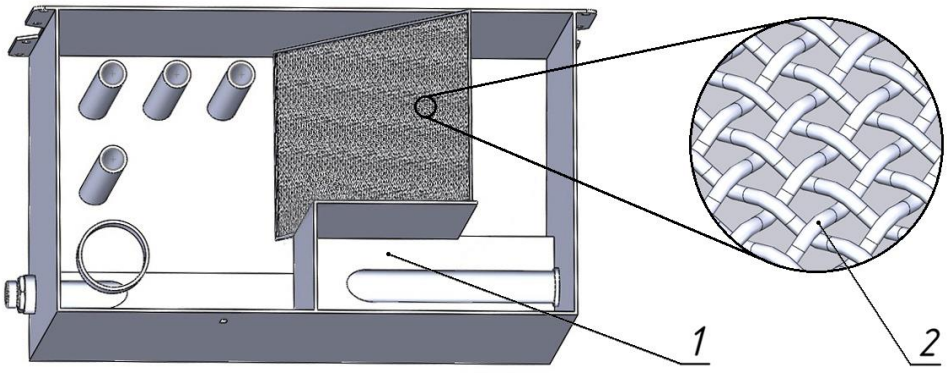

Figure 5. Modified tank design 3dmodel

The ports and functional elements (excepting deaerating inclined screen) location correspond to the initial drawing data. The presented configuration significantly increase fluid path without changing the tank volume. It is recommended to apply a metal grid that in structure is similar to the coarse filter's grid as an inclined screen. The screen should not provide excessive resistance to the fluid flow so grid opening dimensions has been selected taking this into account. The grid screen may also have as

pecialcoating that increases it ability of air finely divided bubbles catching. The fluid flow action provides air bubbles gradually movement to the surface. Thus, it is possible ominimize the air ingress into the suction line. The fluid deaeration is increased. In particular cases at relatively high flow rate through the screen it makes sense put to use several grid layers.

Similar lyper formed (the same boundary conditions) tank's fluid flow simulation results are presented in Fig. 6 and Fig. 7.

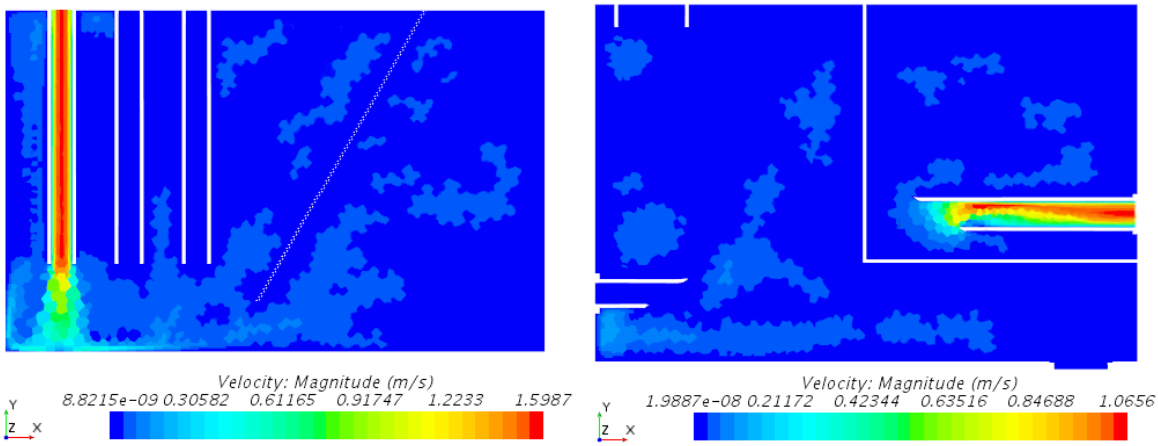

Figure 6. Scalar fields of the velocity distribution over sections A-A (left) and B-B (right)

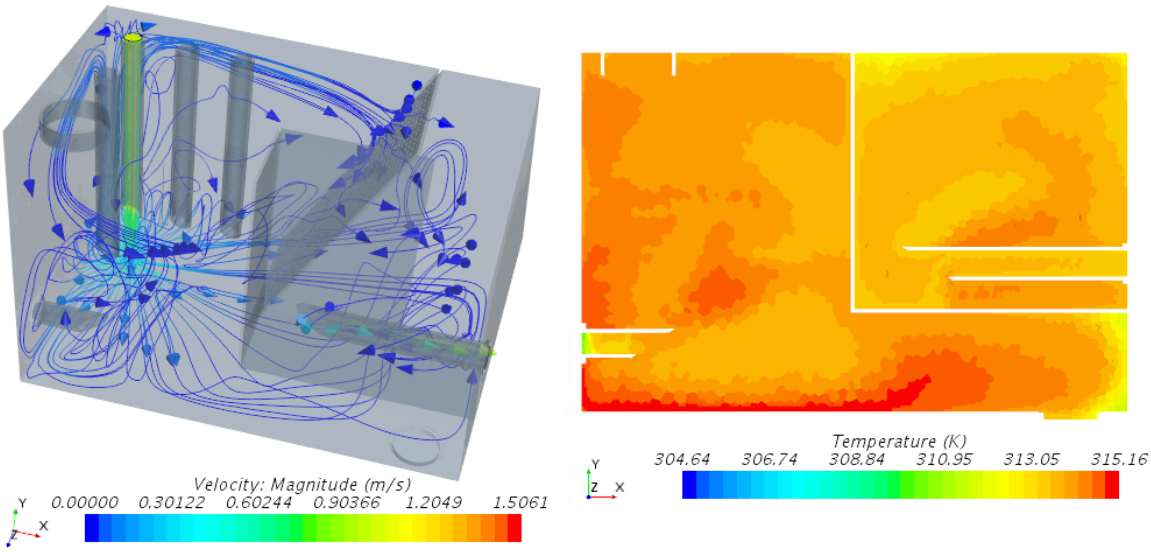

Figure 7. Flow lines (left) and scalar field of the temperature distribution over sectionB-B (right)

In this case before achieve the suction pipe the coming from the return pipe stream flows around additional solid baffles and the residence fluid in the tank time increases. The processes of oil cooling, settling contaminants to the bottom, rising air bubbles to the surface are more intense [9].

Proposed tank design contributes to a more uniform flow velocities distribution and flow lines in the tank volume which positively affects the cooling, deaerating and cleaning reservoir functions [4, 20]. The average fluid temperature is 313,6 K in suction pipe inlet region.

Optimal tank overall l dimensions selecting

Since described above tank design provides al on ger path for the fluid to pass from the return port to the suction port the tank dimensions may be changed to reduce its volume. As an example the large

stoverall dimension is considered — the tank length (marked L dimension in Fig. 1). The task is the selection length value which a flow regime favorable from the point of most efficiency view isobserved. Leng this determined by optimization according to a criterion of the ensuring the most uniform velo city distribution in the fluid volume. The quadratic velocity difference is used to assess the velocity scalar field non-uniformity

$$V_r = \sum_{j=1}^{n} \left(V_j - V_{j+1}\right)^2,$$

where j — fluid volume points index; V_j — velocity value at a point without taking into account flow direction. Sixteen control points $n = 16$ were selected for optimization. Control points are set directly in the fluid volume with the exception suction and return tubes regions. A count of control points may be wider in order to increase accuracy. The results of five consecutive calculations $(i = 1 \ldots 5)$ corresponding to length L variation from 402 mm to 570 mm are presented as a schedule in Fig. 8.

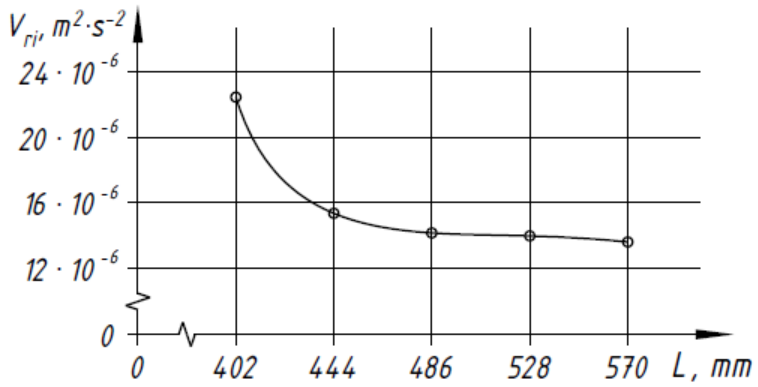

Figure 8. Velocity scalar field uniformity criterion V_{ri} dependence from L dimension value

Selection L value recommend dations have been done based on the obtained results. An intensive increase in unevenness begins with a starting from $L \approx 440$ mm length decrease, the unevenness decrease with an increase in L: the dependence turns out to be similar to hyperbolic. It is not any sense to produce very long tank because that approach provides a relatively low unevenness reduction but its manufacture cost is greatly increased at the same time. In described case is recommended to choose L value from range of 440…480 mm.

Conclusions

Proposed tank design changes contribute to:

- reduction of the tank size in favor of a more efficient contained in it fluid use;
- better removal of contaminants and gas bubbles from the fluid;
- uniform use entire fluid volume and improving tank property heat removal.

The presented simulation procedure and the obtained during study results can be useful for hydrostatic actuator tank development. The main design features that affect the tank functions efficiency are noted.

Reference

[1] Tič, V. &Lovrec, D. 2012. Design of modern hydraulic tank using fluid flow simulation. International Journal of Simulation Modelling, Vol. 11, No. 2, pp. 77–88. https://doi.org/10.2507/IJSIMM11(2)2.202

[2] Singala, V., Bajaj, J., Awalgaonkara, N. &Tibdewalc, S. 2014. CFD Analysis of a kerosene fuel tank to reduce liquid sloshing, Procedia Engineering, Vol. 69, pp. 1365–1371. https://doi.org/10.1016/j.proeng.2014.03.130
[3] Zhang, Ch. 2015. Application of an improved semi-Lagrangian procedure to fully-nonlinear simulation of sloshing in non-wall-sided tanks, Applied Ocean Research 51, 74–92, 2015. https://doi.org/10.1016/j.apor.2015.03.001
[4] Sakama, S., Tanaka, Y., Higashi, H., Goto, H. & Suzuki, R. 2014. Air Bubble Separation and Elimination from Working Fluids for Performance Improvement of Hydraulic Systems. Proc. IFPE 2014, March 4-8, 2014, Las Vegas, USA. 8 p. https://doi.org/10.13140/2.1.4927.4245
[5] Vollmer, T., Untch, J. Capabilities and Challenges of CDF Multiphase Simulation of Hydraulic Tanks. In: *Proceedings of the 8th FPNI Ph.D Symposium on Fluid Power*, Lappeenranta, Finland, June 11–13, 2014. https://doi.org/10.1115/FPNI2014-7849
[6] Wohlers, A., Backes, A. and Schönfeld, D. "An Approach to Optimize the Design of Hydraulic Reservoirs," in 10. InternationalesFluidtechnischesKolloquium, Dresden, 2016.
[7] Močilan, M., Žmindák, M., Pecháč, P. & Weis, P. 2017. CFD Simulation of Hydraulic Tank. ProcediaEngineering, Vol. 192, pp. 609–614. https://doi.org/10.1016/j.proeng.2017.06.105
[8] Ling Hou, Fangcheng Li, Chunliang Wu, A Numerical Study of Liquid Sloshing in Two-dimensional Tank under External Excitations, Journal of Marine Science Applications 11, 305–310, 2012. https://doi.org/10.1007/s11804-012-1137-y
[9] Tič, V.; Lovrec, D. Air-release and Solid Particles Sedimentation Processwithin a Hydraulic Reservoir. // TehničkiVjesnik- Technical Gazette. 20, 3(2013), pp. 407–412.ISSN 1848-6339
[10] Birykov, B.N. Hydraulic equipment for metal cutting machines. M.: Mashinostroenie, 1979. — 112 p.
[11] Salutagi, S., Creswick, M., Yuan, Q., Ding, H. Axial Piston Pump Performance Prediction using 3D CFD Simulation. EatonCorp. SimericsInc. 2015.
[12] RodionovL.V. Features of simulation the gear pump operation process hydrodynamics. Izvestiya Samar. scientific RAN Center. 2017. 19, No 4, part. 1, pp. 15–21.
[13] V Cheremushkin and APolyakov 2019 *IOP Conf. Ser.: Mater. Sci. Eng.***589** 012001
[14] P Chaburko et al 2019 *IOPConf. Ser.: Mater. Sci. Eng.***492** 012011
[15] V Tkachuk et al 2019 *IOP Conf. Ser.: Mater. Sci. Eng.***589** 012007
[16] V Lomakin et al 2019 *IOP Conf. Ser.: Mater. Sci. Eng.***492** 012012
[17] A Boyarshinova et al 2019 *IOP Conf. Ser.: Mater. Sci. Eng.***589** 012014
[18] Wu, C., Xu, C., Mao, X., Li, B., Hu, J. & Liu, Y. 2017. Heating analysis in constant-pressure hydraulic system based on energy analysis. IOP Conf. Series: Earth and Environmental Science, Vol. 100, p. 012147. https://doi.org/10.1088/1755-1315/100/1/012147
[19] Pimonov, G.G., Pimonov, I.G. Research and development of heat-control system for hydraulic actuator. Vestnik HNADU, issue 65–66, 2014.
[20] Rylyakin, E.G. Operation factors influence on the hydraulic actuator technical conditions changes/ Materialy X mezinarodnivedecko-prakticka conference «Modernivymozenostivedy— 2014». —Dil 38. Technickevedy. // Praha. Publishing House «Education and Science». — 2014. — pp. 13–15.